
GraphSAINT: Graph Sampling Based Inductive Learning Method

Hanqing Zeng*

University of Southern California
zengh@usc.edu

Hongkuan Zhou*

University of Southern California
hongkuaz@usc.edu

Ajitesh Srivastava

University of Southern California
ajiteshs@usc.edu

Rajgopal Kannan

US Army Research Lab-West
rajgopal.kannan.civ@mail.mil

Viktor Prasanna

University of Southern California
prasanna@usc.edu

Abstract

Graph Convolutional Networks (GCNs) are powerful models for learning representations of attributed graphs. To scale GCNs to large graphs, state-of-the-art methods use various *layer sampling* techniques to alleviate the “neighbor explosion” problem during minibatch training. Here we propose GraphSAINT, a *graph sampling* based inductive learning method that improves training efficiency in a fundamentally different way. By a change of perspective, GraphSAINT constructs minibatches by sampling the training graph, rather than the nodes or edges across GCN layers. Each iteration, a complete GCN is built from the properly sampled subgraph. Thus, we ensure fixed number of well-connected nodes in all layers. We further propose normalization technique to eliminate bias, and sampling algorithms for variance reduction. Importantly, we can decouple the sampling process from the forward and backward propagation of training, and extend GraphSAINT with other graph samplers and GCN variants. Comparing with strong baselines using layer sampling, GraphSAINT demonstrates superior performance in both accuracy and training time on four large graphs.

1 Introduction

Recently, representation learning on graphs has attracted much attention, since it greatly facilitates tasks such as classification and clustering [30, 4]. Current works on Graph Convolutional Networks (GCNs) [14, 6, 9, 18, 5] mostly focus on shallow models (2 layers) on relatively small graphs. Scaling GCNs to larger datasets and deeper layers still requires fast alternate training methods.

In a GCN, the data that need to be gathered for one output node comes from its neighbors in the previous layer. Each of these neighbors in turn, gathers its output from the previous layer, and so on. It is easy to see that the deeper we back track, the more multi-hop neighbors we need to support the computation of the root. The number of support nodes (and thus the training time) can grow exponentially with the GCN depth. To mitigate such “neighbor explosion”, state-of-the-art methods [14, 6, 5, 33, 18] use various *layer sampling* techniques. The works in [14, 33, 5] ensure that only a

*Equal contribution

small number of neighbors (typically from 2 to 50) are selected by one node in the next layer. The works in [6, 18] further propose samplers that ensure a fixed number of samples in all layers, which potentially restricts the neighbor expansion factor to 1. While these methods significantly speed up training, they still face various challenges in scalability, accuracy and training complexity.

Present work We present GraphSAINT (Graph SAMpling based INductive learning meThod), an approach for efficient training of deep GCNs. GraphSAINT is developed from a fundamentally different way of minibatch construction. Instead of building a GCN on the complete training graph and then sampling across the layers, we sample the training graph first and then build a full GCN on the subgraph. Our minibatches are thus *graph sampling* based. Naturally, GraphSAINT resolves the challenge of “neighbor explosion” in training, since every GCN we build from the minibatch is a small and *complete* one. To ensure high training accuracy, proper graph samplers need to be developed. Intuitively, nodes having strong influence on each other should be selected in the same subgraph. This way, when propagating through the GCN layers, the sampled nodes can “support” each other without gathering information from outside the batch. Through insights gathered from theoretical analysis, we propose several simple graph samplers that lead to fast and highly accurate training. Accompanied with the graph sampling idea, we also develop normalization and variance reduction techniques to further improve training quality. Experiments demonstrate that GraphSAINT achieves highest accuracy in shortest training time, compared with several strong baselines on four large graphs. On the Reddit dataset, we achieve 9× training time reduction with higher accuracy.

2 Related Work

A neural network model that extends convolution operation to graph domain is first proposed by the pioneer work in [3]. The works in [20, 8] further speed up graph convolution computation by fast localized filters based on Chebyshev expansion. They target relatively small datasets and thus the training proceeds in full batch. In order to scale GCNs to large graphs, layer sampling techniques [14, 6, 33, 5, 9, 18] have been proposed for efficient minibatch training. All of them follow the three meta steps: 1. Construct a complete GCN on the full training graph. 2. Sample nodes or edges of each layer to construct minibatches. 3. Propagate forward and backward among the sampled GCN. Steps (2) and (3) proceed iteratively to update the weights via stochastic gradient descent. The layer sampling algorithm proposed by GraphSAGE [14] performs uniform node sampling on the neighbors lying in the previous layer. It enforces a pre-defined budget on sampled neighbors, so as to bound the complexity of minibatch execution. The work in [33] enhances the layer sampler of [14] by introducing an importance score to each neighbor node. The algorithm presumably leads to less information loss due to its preference towards influential neighbors. To further restrict the neighborhood size of deep layers, [5] requires only two neighbors to support the computation of next layer activations. The idea is to use the historical activations in the previous layer to avoid redundant re-evaluation. FastGCN [6] performs sampling from another perspective. Instead of tracking down the inter-layer connections to construct minibatches, node sampling is performed independently for each layer. They apply importance sampling for explicit variance reduction, and remarkably, their method leads to constant number of samples in all layers. However, their minibatches potentially become too sparse to achieve high accuracy. The work in [18] improves [6] by adding an additional sampling neural network. It ensures high accuracy as well as constant neighborhood size, since sampling is conditioned on the selected nodes in the next layer. Significant overhead may be incurred due to the complicated sampling mechanism and the extra sampler parameters to be learned. In addition, the work in [35] proposes a subgraph based training algorithm that is scalable with respect to GCN depth, and also highly parallelizable on multi-core machines. More recent work [7] builds minibatches based on (topological) clusters of the training graph, and shows the effectiveness of their algorithm on deep models. While the subgraph based methods [35, 7] empirically demonstrate high node classification accuracy, their minibatches inherently result in biased estimation of the full batch loss. Thus, more analysis may be required to understand their convergence property.

Another line of research focuses on improving GCN model capacity. Applying the attention mechanism on graphs, GAT [29] better captures neighbor features by adjusting edge weights. [21] combines PageRank with GCNs to enable efficient information propagation from many hops away. To develop deeper GCN models, the “skip-connection” idea is borrowed from CNNs [15] into the GCN context [18, 9, 31]. In particular, JK-Net [31] demonstrates significant accuracy improvement on GCNs with more than two layers. It should be noted, however, that JK-Net [31] follows the same

sampling strategy as GraphSAGE [14]. Thus, its training cost is still high due to neighbor explosion. In addition to the above works that provide inter-layer shortcut connection, high order graph convolutional layers [36, 22, 2] have also been used to help propagate long-distance features. With the numerous GCN variants developed, it still remains a question how to train these models efficiently via minibatches.

3 Proposed Method: GraphSAINT

Graph sampling based method is motivated by its resolution of “neighbor explosion” in minibatch training. We analyze in detail the bias (Section 3.2) and variance (Section 3.3) introduced by graph sampling, and thus, recommend feasible sampling algorithms (Section 3.4). We also demonstrate the general applicability of GraphSAINT to other models, and differentiate ourselves with existing layer sampling based methods in several ways (Section 4).

Below we define the problem of interest and the corresponding notations. A GCN learns representation of an un-directed, attributed graph $\mathcal{G}(\mathcal{V}, \mathcal{E})$, where each node $v \in \mathcal{V}$ has a length- f attribute \mathbf{x}_v . Let \mathbf{A} be the adjacency matrix and $\tilde{\mathbf{A}}$ be the normalized one (i.e., $\tilde{\mathbf{A}} = \mathbf{D}^{-1}\mathbf{A}$, and \mathbf{D} is the diagonal degree matrix). Let the dimension of layer- ℓ input activation be $f^{(\ell)}$. The activation of node v is $\mathbf{x}_v^{(\ell)} \in \mathbb{R}^{f^{(\ell)}}$, and the weight matrix is $\mathbf{W}^{(\ell)} \in \mathbb{R}^{f^{(\ell)} \times f^{(\ell+1)}}$. Note that $\mathbf{x}_v = \mathbf{x}_v^{(1)}$. Propagation rule of a layer is defined as follows:

$$\mathbf{x}_v^{(\ell+1)} = \sigma \left(\sum_{u \in \mathcal{V}} \tilde{\mathbf{A}}_{v,u} (\mathbf{W}^{(\ell)})^T \mathbf{x}_u^{(\ell)} \right) \quad (1)$$

where $\tilde{\mathbf{A}}_{v,u}$ is a scalar, taking an element of $\tilde{\mathbf{A}}$, and $\sigma(\cdot)$ is the activation function (e.g., ReLU).

Note that in the following sections, we use subscript “s” to denote a parameter of the sampled graph.

GCNs can be applied under inductive as well as transductive settings. While GraphSAINT is applicable to both, in this paper, we focus on inductive learning. It has been shown that inductive learning is especially difficult [14] — during training, neither the attributes nor the connections of the test nodes are present. Thus, an inductive GCN model has to generalize to completely unseen graphs.

3.1 Minibatch by Graph Sampling

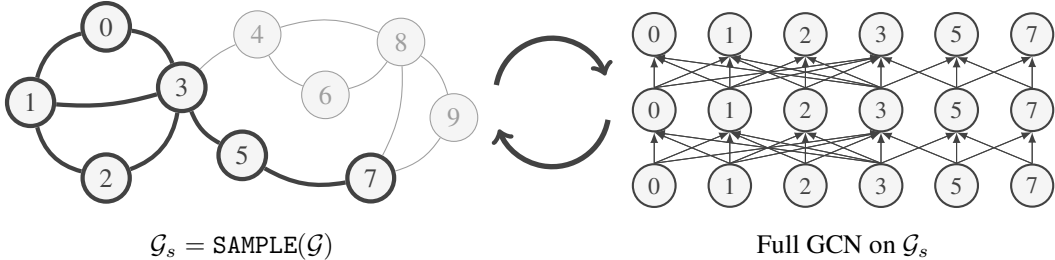


Figure 1: GraphSAINT training algorithm

GraphSAINT follows the design philosophy of directly sampling the training graph \mathcal{G} , rather than the corresponding GCN. Intuitively, using proper graph sampling algorithms, we can extract small representative subgraphs from the large training graph, such that accurate node embedding can be obtained by propagating information *within the subgraphs*.

Figure 1 and Algorithm 1 illustrate the overall training algorithm. Before training starts, we perform light weight pre-processing on \mathcal{G} with the given sampler SAMPLE. The pre-processing estimates the probability of a node $v \in \mathcal{V}$ and an edge $e \in \mathcal{E}$ being sampled by SAMPLE. Such probability is later used to normalize the subgraph neighbor aggregation and the minibatch loss (Section 3.2). After pre-processing, training proceeds by iterative weight updates via SGD. Each iteration starts with an independently sampled \mathcal{G}_s (where $|\mathcal{V}_s| \ll |\mathcal{V}|$). We then build a full GCN on \mathcal{G}_s to generate

Algorithm 1 GraphSAINT training algorithm

Input: Training graph $\mathcal{G}(\mathcal{V}, \mathcal{E}, \mathbf{X})$; Labels $\overline{\mathbf{Y}}$; Sampler SAMPLE;**Output:** GCN model with trained weights

- 1: Pre-processing: Setup SAMPLE parameters; Compute normalization coefficients α, λ .
 - 2: **for** each minibatch **do**
 - 3: $\mathcal{G}_s(\mathcal{V}_s, \mathcal{E}_s) \leftarrow$ Sampled sub-graph of \mathcal{G} according to SAMPLE
 - 4: GCN construction on \mathcal{G}_s .
 - 5: $\{\mathbf{y}_v \mid v \in \mathcal{V}_s\} \leftarrow$ Forward propagation of $\{\mathbf{x}_v \mid v \in \mathcal{V}_s\}$, normalized by α
 - 6: Backward propagation from λ -normalized loss $L(\mathbf{y}_v, \overline{\mathbf{y}}_v)$. Update weights.
 - 7: **end for**
-

embedding for every $v \in \mathcal{V}_s$. We calculate loss by regarding every $v \in \mathcal{V}_s$ as the minibatch node. In Algorithm 1, node representation is learned by performing node classification in the supervised setting, and each training node v comes with a ground truth label $\overline{\mathbf{y}}_v$.

One would naturally wonder how to design the function SAMPLE. Intuitively, there are two requirements: 1. Nodes that have high influence on each other should be sampled in the same sub-graph. 2. Each edge should have non-negligible probability to be sampled. For requirement (1), an ideal SAMPLE would consider the joint information from node connections as well as attributes. However, the resulting algorithm may have high complexity as it would need to infer the relationships between features. For simplicity, it is reasonable to define ‘‘influence’’ from the graph connectivity perspective and design topology based samplers. Requirement (2) leads to better generalization since the neural net can explore the whole feature and label space without high sample complexity.

3.2 Normalization

A sampler that preserves connectivity characteristic of \mathcal{G} will almost inevitably introduce bias into minibatch estimation. Below we present normalization techniques to eliminate biases. Analysis of the whole multi-layer GCN is difficult due to non-linear activations. Thus, we analyze the embedding of each layer independently. Consider a layer- $(\ell + 1)$ node v and a layer- ℓ node u . If v is sampled (i.e., $v \in \mathcal{V}_s$), we can compute the aggregated feature of v as:

$$\zeta_v^{(\ell+1)} = \sum_{u \in \mathcal{V}} \frac{\tilde{\mathbf{A}}_{v,u}}{\alpha_{u,v}} \left(\mathbf{W}^{(\ell)} \right)^T \mathbf{x}_u^{(\ell)} \mathbb{1}_{u|v} = \sum_{u \in \mathcal{V}} \frac{\tilde{\mathbf{A}}_{v,u}}{\alpha_{u,v}} \tilde{\mathbf{x}}_u^{(\ell)} \mathbb{1}_{u|v}, \quad (2)$$

where $\tilde{\mathbf{x}}_u = \left(\mathbf{W}^{(\ell)} \right)^T \mathbf{x}_u^{(\ell)}$, and $\mathbb{1}_{u|v} \in \{0, 1\}$ is the indicator function given that v is in the subgraph (i.e., $\mathbb{1}_{u|v} = 0$ if $v \in \mathcal{V}_s \wedge (u, v) \notin \mathcal{E}_s$; $\mathbb{1}_{u|v} = 1$ if $(u, v) \in \mathcal{E}_s$; $\mathbb{1}_{u|v}$ not defined if $v \notin \mathcal{V}_s$). Note that $\alpha_{u,v}$ is a constant that we refer to as *aggregator normalization*.

Define $p_{u,v} = p_{v,u}$ as the probability of an edge $(u, v) \in \mathcal{E}$ being sampled in a subgraph, and p_v as the probability of a node $v \in \mathcal{V}$ being sampled in a subgraph. Then,

Proposition 3.1. $\zeta_v^{(\ell+1)}$ is an unbiased estimator of the aggregation of v in full GCN, if $\alpha_{u,v} = \frac{p_{u,v}}{p_v}$, i.e.,

$$\mathbb{E} \left(\zeta_v^{(\ell+1)} \right) = \sum_{u \in \mathcal{V}} \tilde{\mathbf{A}}_{v,u} \tilde{\mathbf{x}}_u^{(\ell)}$$

Further, let L_v be the loss on v in the output layer. The minibatch loss is calculated as $L_{\text{batch}} = \sum_{v \in \mathcal{G}_s} L_v / \lambda_v$, where λ_v is a constant that we term *loss normalization*. We set $\lambda_v = |\mathcal{V}| \cdot p_v$ so that:

$$\mathbb{E} (L_{\text{batch}}) = \frac{1}{|\mathcal{V}|} \sum_{\mathcal{G}_s} \sum_{v \in \mathcal{V}_s} \frac{L_v}{p_v} = \frac{1}{|\mathcal{V}|} \sum_{v \in \mathcal{V}} L_v. \quad (3)$$

Feature propagation within subgraphs thus requires normalization factors α and λ , which are computed based on the edge and node probability $p_{u,v}, p_v$. In the case of random node or random edge samplers, $p_{u,v}$ and p_v can be derived analytically. For other samplers in general, closed form expression is hard to obtain. Thus, we perform pre-processing for estimation. Before training starts, we run the sampler repeatedly to obtain a set of N subgraphs \mathbb{G} . We setup a counter C_v and $C_{u,v}$ for

each $v \in \mathcal{V}$ and $(u, v) \in \mathcal{E}$, to count the number of times the node or edge appears in the subgraphs of \mathbb{G} . Then we set $\alpha_{u,v} = \frac{C_{u,v}}{C_v} = \frac{C_{v,u}}{C_v}$ and $\lambda_v = \frac{C_v}{N}$. The subgraphs $\mathcal{G}_s \in \mathbb{G}$ can all be reused as minibatches during training. Thus, the overhead of pre-processing is small (see Section 5.2).

3.3 Variance

We derive samplers for variance reduction. Let e be the edge connecting u, v , and $b_e^{(\ell)} = \tilde{\mathbf{A}}_{v,u} \tilde{\mathbf{x}}_u^{(\ell-1)} + \tilde{\mathbf{A}}_{u,v} \tilde{\mathbf{x}}_v^{(\ell-1)}$. It is desirable that variance of all estimators $\zeta_v^{(\ell)}$ is small. With this objective, we define:

$$\zeta = \sum_{\ell} \sum_{v \in \mathcal{G}_s} \frac{\zeta_v^{(\ell)}}{p_v} = \sum_{\ell} \sum_{v,u} \frac{\tilde{\mathbf{A}}_{v,u}}{p_v \alpha_{u,v}} \tilde{\mathbf{x}}_u^{(\ell)} \mathbb{1}_v \mathbb{1}_{u|v} = \sum_{\ell} \sum_e \frac{b_e^{(\ell)}}{p_e} \mathbb{1}_e^{(\ell)}. \quad (4)$$

where $\mathbb{1}_e = 1$ if $e \in \mathcal{E}_s$; $\mathbb{1}_e = 0$ if $e \notin \mathcal{E}_s$. And $\mathbb{1}_v = 1$ if $v \in \mathcal{V}_s$; $\mathbb{1}_v = 0$ if $v \notin \mathcal{V}_s$. The factor p_u in the first equality is present so that ζ is an unbiased estimator of the sum of all node aggregations at all layers: $\mathbb{E}(\zeta) = \sum_{\ell} \sum_{v \in \mathcal{V}} \mathbb{E}(\zeta_v^{(\ell)})$. Note that $\mathbb{1}_e^{(\ell)} = \mathbb{1}_e, \forall \ell$, as once an edge is present in the sampled graph, it is present in all layers of our GCN.

Below we define the optimal edge sampler to minimize the variance of ζ . We restrict ourselves to independent edge sampling. For each $e \in \mathcal{E}$, we make independent decision on whether it should be included in \mathcal{G}_s or not. The probability of including e is p_e . We further constrain $\sum p_e = m$, so that the expected number of sampled edges equals to m . The budget m is a given sampling parameter.

Theorem 3.2. *Under independent edge sampling of budget m , the optimal edge probabilities for minimizing the variance of ζ is given by $p_e = \frac{m}{\sum_{e', \ell} b_{e'}^{(\ell)}} \sum_{\ell} b_e^{(\ell)}$.*

To prove Theorem 3.2, we make use of the independence among graph edges, and the dependence among layer edges to obtain the covariance of $\mathbb{1}_e^{(\ell)}$. Then using the fact that sum of p_e is a constant, we use the Cauchy-Schwarz inequality to derive the optimal p_e . Details are in Appendix A.

Note that calculating $b_e^{(\ell)}$ requires computing $\tilde{\mathbf{x}}_v^{(\ell-1)}$, which increases the complexity of sampling. As a reasonable simplification, we ignore $\tilde{\mathbf{x}}_v^{(\ell)}$ to make the edge probability dependent on the graph only. Therefore, we choose $p_e \propto \tilde{\mathbf{A}}_{v,u} + \tilde{\mathbf{A}}_{u,v} = \frac{1}{\deg(u)} + \frac{1}{\deg(v)}$.

The derived optimal edge sampler agrees with the intuition in Section 3.1. If two nodes u, v are connected and they have few neighbors, then u and v are likely to be influential to each other. In this case, the edge probability $p_{u,v} = p_{v,u}$ should be high. The above analysis on edge samplers also inspires us to design other samplers, which are presented in Section 3.4.

Remark We can also apply the above edge sampler to perform layer sampling. Under the independent layer sampling assumption of [6], one would sample a connection $(u^{(\ell)}, v^{(\ell+1)})$ with probability $p_{u,v}^{(\ell)} \propto \frac{1}{\deg(u)} + \frac{1}{\deg(v)}$. For simplicity, assume a uniform degree graph (of degree d). Then $p_e = p$. For an already sampled $u^{(\ell)}$ to connect to layer $\ell + 1$, at least one of its edges has to be selected by the layer $\ell + 1$ sampler. Clearly, the probability of an input layer node to “survive” the L number of independent sampling process is $(1 - (1 - p)^d)^{L-1}$. Such layer sampler potentially returns an overly sparse minibatch for $L > 1$. On the other hand, connectivity within a minibatch of GraphSAINT never drops with GCN depth. If an edge is present in layer ℓ , it is present in all layers.

3.4 Samplers

Below we describe several simple and efficient samplers that GraphSAINT has integrated.

Random node sampler Each time, we sample $|\mathcal{V}_s|$ nodes from \mathcal{V} randomly, according to a node probability distribution $P(u) \propto \|\tilde{\mathbf{A}}_{:,u}\|^2$. This sampler is similar to the layer sampler in [6].

Random edge sampler We perform edge sampling as described in Section 3.3.

Random walk based samplers Another way to analyze graph sampling based multi-layer GCN is to ignore activations. In that case, L layers can be represented as a single layer with edge weights given by $B = \tilde{A}^L$. Following a similar approach as Section 3.3, if it were possible to pick pairs of nodes independently with probability $p_{u,v}^{(L)}$ then we would set $p_{u,v}^{(L)} \propto B_{u,v} + B_{v,u}$. It can be observed that $B_{u,v}$ is the probability of a random walk to start at u and end at v in L hops, and $B_{v,u}$ vice-versa. Even though it is not possible to sample a subgraph where such pairs of nodes are independently selected, we still consider a random walk sampler with walk length L as a good candidate sampler for L -layer GCNs. There are many random walk based samplers in the literature [26, 23, 17, 24]. In the experiments, we implement a regular random walk sampler (with r root nodes selected uniformly at random and each walker goes h hops), and also a multi-dimensional random walk sampler [26].

For all the above samplers, we return the subgraph induced from the sampled nodes. The induction step adds more edges into the subgraph, and empirically helps improve accuracy. Detailed sampling algorithms are listed in Appendix B.

4 Discussion

Extensions GraphSAINT can be extended in various ways. One natural extension is to integrate other samplers based on the graph characteristics. More importantly, the idea of training by graph sampling is applicable to many GCN variants. To support attention mechanism [29], while explicit variance reduction is hard due to the dynamically updated attention values, it is still reasonable to apply attention within the subgraphs which are representatives of the full graph. The loss and aggregator normalizations are also applicable with attention. To support high order layers [36, 22, 2], skip-connection [15, 18, 31] or even more complicated networks such as [34], it is sufficient to replace the full adjacency matrix A with the one for the subgraph A_s to perform layer propagation.

Comparison GraphSAINT differentiates itself from other layer sampling based methods. Graph sampling naturally leads to: 1. constant neighborhood size in all layers, 2. good inter-layer connectivity among minibatch nodes, and 3. small training overhead introduced by sampling. Point (1) improves training efficiency and scalability by resolving “neighbor explosion” in [14, 5, 33]. Point (2) improves accuracy and robustness on sparse graphs and deep nets by avoiding the overly sparse minibatches of [6] (see Section 3.3). Point (3) reduces training time by decreasing the number of sampler invocations (compared with [6, 18]), and the cost of each invocation (compared with [18]).

5 Experiments

Setup We conduct experiments under the inductive, supervised learning setting. As shown in Table 1, we evaluate four large graph datasets. 1. *Protein-Protein Interaction (PPI) graph* [27]: The features correspond to positional gene sets, motif gene sets and immunological signatures [37]. The labels are gene ontology sets. 2. *Flickr graph* [28]: A node represents an image on Flickr, and an edge presents if the nodes share the same location, gallery, etc. Node features contain the bag of words representation of the image description. The labels categorize the type of the image (such as portrait or nature scene). 3. *Reddit graph* [27]: A node represents a post on Reddit, and an edge is formed if the nodes shared a common user in their comments. The node features are the concatenation of word vectors of their title and comments. The labels are the community (on Reddit) of the posts. 4. *Yelp graph* [32]: A node represents a user of Yelp. An edge represents friendship. The node features are word embeddings from the user reviews. The labels indicate the types of businesses that the user has reviewed. All four datasets follow “fixed-partition” splits. Appendix C.2 includes further details.

We implement graph samplers in Python and the training algorithm in Tensorflow [1] (open-sourced*). We run experiments on a NVIDIA Tesla P100 GPU (see Appendix C.1 for hardware specification).

*<https://github.com/GraphSAINT/GraphSAINT>

Table 1: Dataset statistics (“m” stands for **multi-class classification**, and “s” for **single-class**.)

Dataset	Nodes	Edges	Degree	Feat.	Classes	Train / Val / Test
PPI	14,755	225,270	15	50	121 (m)	0.66 / 0.12 / 0.22
Flickr	89,250	899,756	10	500	7 (s)	0.50 / 0.25 / 0.25
Reddit	232,965	11,606,919	50	602	41 (s)	0.66 / 0.10 / 0.24
Yelp	716,847	6,977,410	10	300	100 (m)	0.75 / 0.10 / 0.15

5.1 Comparison with State-of-the-Art

We compare GraphSAINT with five baselines using layer sampling: 1. The vanilla GCN [20] (with its batched implementation at [12]); 2. GraphSAGE [14] with uniform neighbor sampling (released code: [12]); 3. FastGCN [6] with importance sampling (released code: [11]); 4. S-GCN [5] with control variate based variance reduction (released code: [13]); 5. AS-GCN [18] with auxiliary neural network based sampler (released code: [10]). For GraphSAINT, we implement the graph samplers described in Section 3.4. In Table 2, “Node” stands for random node sampler; “Edge” stands for random edge sampler; “RW” stands for random walk sampler; “MRW” stands for multi-dimensional random walk sampler. The corresponding edge or node probability is specified in Section 3.4.

All results in Table 2 are based on 2-layer GCN models (for [14], we use GraphSAGE-mean). Given a dataset, we keep the hidden dimensions the same for all baselines and GraphSAINT. Testing and validation accuracy (F1-micro score) are all obtained by running the full GCN without any sampling. We use batch size of 512 for [20, 14, 18], 1000 for [5], and 400 for [6]. For GraphSAINT, batch size (i.e., subgraph size) depends on the specific sampler. See Appendix E for graph sampler parameters, and additional experiments on evaluating the baselines with larger batch size. The “Time” in Table 2 measures training time until termination (specifically, GPU execution time for [20, 14, 5, 18] and GraphSAINT; CPU execution time for [6]). We exclude the time for data loading, pre-processing and Tensorflow model saving. See Section 3.4 for discussion on pre-processing cost.

Table 2: Comparison of test set accuracy and training time with state-of-the-art methods

Method	PPI		Flickr		Reddit		Yelp	
	F1 _{mic}	Time (s)	F1 _{mic}	Time (s)	F1 _{mic}	Time (s)	F1 _{mic}	Time (s)
GCN [20]	0.515	13	0.472	11	0.933	36	0.378	170
GraphSAGE [14]	0.637	35	0.389	5	0.953	26	0.634	161
FastGCN [†] [6]	0.513	7	0.504	82	0.924	400	0.265	744
S-GCN [5]	0.963	40	0.464	8	0.964	119	0.640	117
AS-GCN [18]	0.687	36	0.504	169	0.958	659	— [‡]	— [‡]
GraphSAINT-Node	0.960	47	0.507	5	0.962	15	0.641	183
GraphSAINT-Edge	0.981	58	0.510	4	0.966	14	0.654	255
GraphSAINT-RW	0.981	61	0.511	4	0.966	13	0.654	343
GraphSAINT-MRW	0.980	59	0.510	3	0.964	12	0.652	370

Accuracy and training time From Table 2, clearly, with appropriate graph samplers, GraphSAINT quickly achieves the highest accuracy on all datasets. GraphSAINT achieves significantly better accuracy than FastGCN [6] due to better inter-layer connectivity among minibatch nodes. GraphSAINT achieves orders of magnitude reduction in training time than AS-GCN [18] due to the extremely light-weight sampling process. Note that for “GraphSAINT-Node”, we use the same node probability as FastGCN. Thus, the accuracy improvement is mainly due to the switching from *layer sampling* to *graph sampling*. For the other two baselines [14, 5], their sampled neighborhood sizes potentially grow exponentially with the GCN depth. Compared with GraphSAGE [14], GraphSAINT using any of the four samplers achieves significantly higher accuracy. Compared with S-GCN [5], GraphSAINT using edge or random walk sampler achieves significantly higher accuracy

[†]The code [11] runs on CPU only, and does not support GPU execution.

[‡]The code [10] throws runtime error on Yelp.

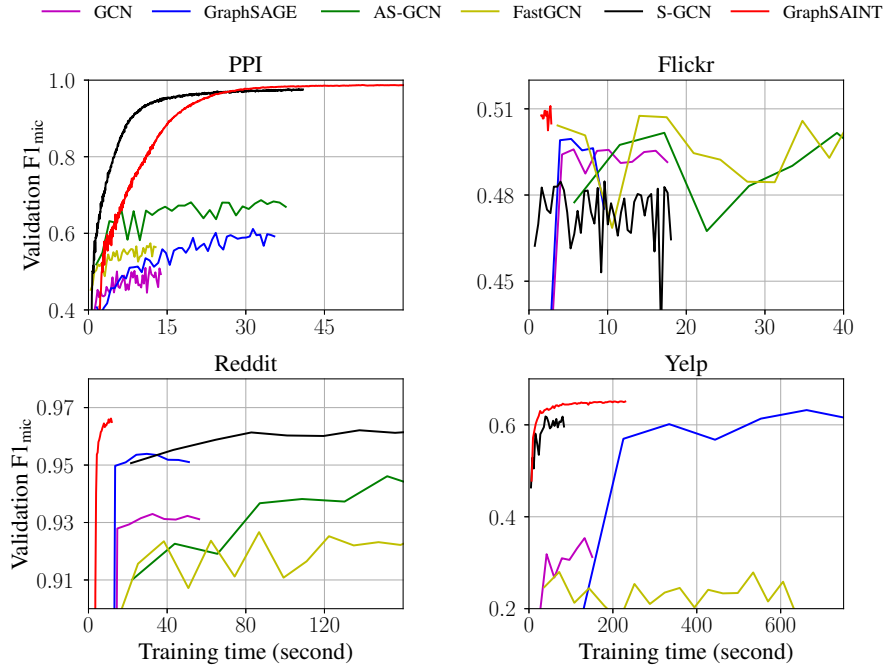


Figure 2: Convergence curves of 2-layer GCNs on GraphSAINT and baselines

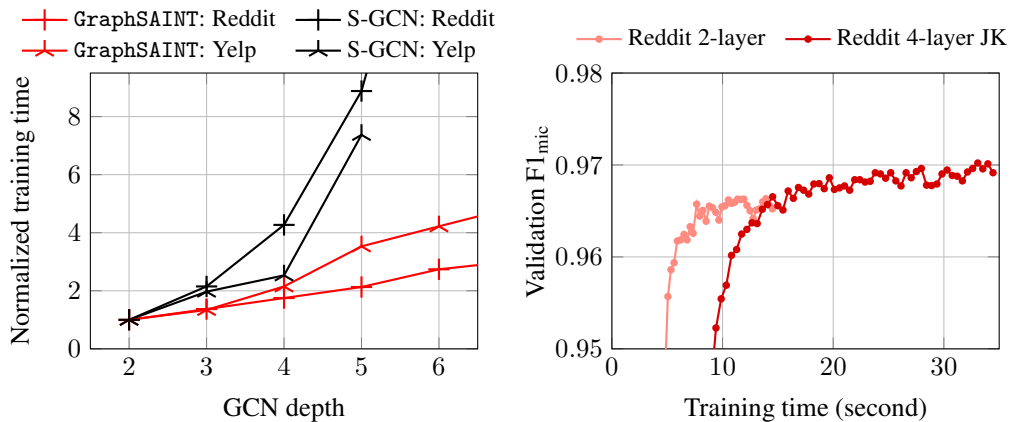


Figure 3: Comparison of training efficiency Figure 4: Training GraphSAINT on deep models

on PPI, Flickr and Yelp, and slightly better accuracy on Reddit. Note that GraphSAINT reduces training time of Reddit by more than $9\times$. Figure 2 shows the convergence curves of all methods. The x -axis is training time, and the y -axis is validation set F1-micro score. The GraphSAINT curves of PPI, Flickr and Reddit correspond to the RW sampler, and the GraphSAINT curve of Yelp corresponds to the edge sampler. Again, we observe GraphSAINT achieves the best training quality.

Training efficiency We further evaluate the training efficiency for deeper GCNs. We only compare with S-GCN since other baseline implementations have not yet supported arbitrarily deep models. The batch size and hidden dimension are the same as Table 2. On the two larger graphs (Reddit and Yelp), we increase the number of layers and measure the average time per minibatch execution. In Figure 3, training cost of GraphSAINT is approximately linear with GCN depth. Training cost of S-GCN grows dramatically when increasing the depth. This reflects the “neighbor explosion”

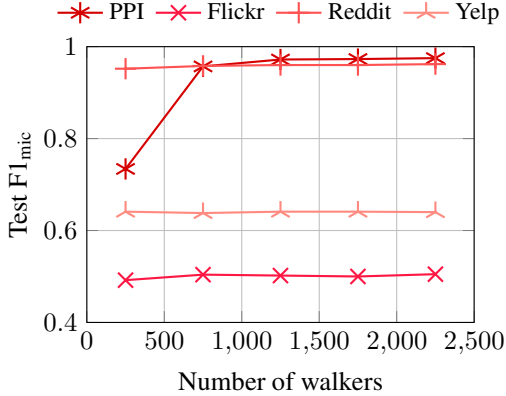


Figure 5: Sensitivity analysis on RW sampler

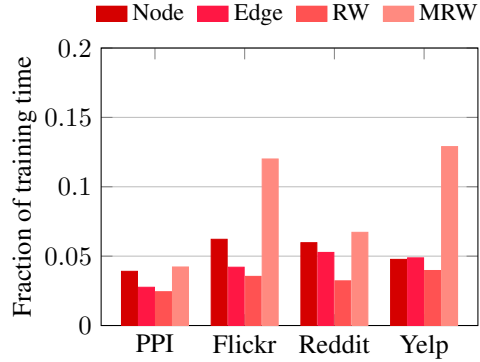


Figure 6: Fraction of training time on sampling

phenomenon. On Yelp, S-GCN gives “out-of-memory” error for models beyond 5 layers. Note that deeper GCNs may require additional training techniques and architectural designs such as skip-connection [15, 31]. Thus, detailed accuracy evaluation is out of scope. In Section 5.3, we also provide accuracy evaluation of an example deep GCN trained with minibatches of GraphSAINT.

5.2 Evaluation on Graph Samplers

From Table 2, random edge and random walk based samplers achieve higher accuracy than the random node sampler. Figure 5 presents sensitivity analysis on parameters of “RW”. We use the same hyperparameters (except the sampling parameters) and network architecture as those of the “RW” experiments in Table 2. We fix the length of each walker to 2 (GCN depth), and vary the number of roots r (from 250 to 2250). For PPI, increasing r from 250 to 750 significantly improves accuracy. Overall, for all datasets, accuracy stabilizes beyond $r = 750$.

Graph sampling introduces little training overhead. Under the same sampling parameters as Table 2, we observe from Figure 6 that, time to sample one subgraph is in most cases less than 10% of the time on one pass of forward plus backward propagation. As for the pre-processing step, we repeatedly run the sampler for $N = 50 \cdot |\mathcal{V}| / \overline{|\mathcal{V}_s|}$ times before training, to estimate the node and edge probability (where $\overline{|\mathcal{V}_s|}$ is the average subgraph size). These sampled subgraphs are reused as training minibatches. Thus, if training runs for more than N iterations, the pre-processing is nearly zero-cost. In our case, pre-processing on PPI and Yelp does not incur extra overhead. Pre-processing on Flickr and Reddit is less than 10% of their corresponding total training time.

5.3 GraphSAINT on GCN Architecture Variants

As discussed in Section 4, the minibatches constructed by graph sampling can be used to efficiently train deeper models, as well as other GCN architecture variants. We integrate the jumping knowledge network (JK-Net) [31] into the GraphSAINT framework, and evaluate the performance of a deep JK-Net trained by minibatches of subgraphs. Figure 4 shows the convergence curves of a 2-layer GCN (defined by Equation 1; hidden dimension 128) and a 4-layer JK-Net (defined in Appendix D; hidden dimension 128), both trained under the edge sampler. The 2-layer GCN achieves 0.966 F1-micro score, while the 4-layer JK-Net achieves over 0.970 F1-micro score. Notably, the training time of the 4-layer model is only around twice that of the 2-layer model. Under the setting of the original JK-Net paper [31], the minibatch training uses the neighbor sampling of GraphSAGE [14], and achieves 0.965 F1-micro for a 2-layer model (hidden dimension 128). However, such training of [31] can not scale to deeper networks. The above results demonstrate that training based on the sampling of GraphSAINT can be applied to other GCN architecture variants, to greatly improve their training efficiency without compromising accuracy.

6 Conclusion

We have presented GraphSAINT, a graph sampling based training method for deep GCNs on large graphs. We have analyzed bias and variance of the minibatches defined on subgraphs, and proposed normalization techniques and sampling algorithms to improve training quality. We have conducted extensive experiments to demonstrate the advantage of GraphSAINT in accuracy and training time. An interesting future direction is to develop distributed training algorithms using graph sampling based minibatches. The graph sampling naturally partitions data, and training on the self-contained subgraphs can significantly reduce the communication cost. Especially, since the graph data may reside on geographically dispersed computation nodes, the property that graph sampling is decoupled from the training helps parallelization, and suits very well in distributed computing environments.

References

- [1] Martín Abadi, Ashish Agarwal, Paul Barham, Eugene Brevdo, Zhifeng Chen, et al. Tensorflow: Large-scale machine learning on heterogeneous distributed systems. *CoRR*, abs/1603.04467, 2016.
- [2] Sami Abu-El-Haija, Bryan Perozzi, Amol Kapoor, Hrayr Harutyunyan, Nazanin Alipourfard, Kristina Lerman, Greg Ver Steeg, and Aram Galstyan. Mixhop: Higher-order graph convolution architectures via sparsified neighborhood mixing. *arXiv preprint arXiv:1905.00067*, 2019.
- [3] Joan Bruna, Wojciech Zaremba, Arthur Szlam, and Yann LeCun. Spectral networks and locally connected networks on graphs. *CoRR*, abs/1312.6203, 2013.
- [4] HongYun Cai, Vincent W. Zheng, and Kevin Chen-Chuan Chang. A comprehensive survey of graph embedding: Problems, techniques and applications. *CoRR*, abs/1709.07604, 2017.
- [5] Jianfei Chen, Jun Zhu, and Le Song. Stochastic training of graph convolutional networks with variance reduction. In *ICML*, pages 941–949, 2018.
- [6] Jie Chen, Tengfei Ma, and Cao Xiao. Fastgcn: Fast learning with graph convolutional networks via importance sampling. In *International Conference on Learning Representations (ICLR)*, 2018.
- [7] Wei-Lin Chiang, Xuanqing Liu, Si Si, Yang Li, Samy Bengio, and Cho-Jui Hsieh. Cluster-gcn: An efficient algorithm for training deep and large graph convolutional networks. *CoRR*, abs/1905.07953, 2019.
- [8] Michaël Defferrard, Xavier Bresson, and Pierre Vandergheynst. Convolutional neural networks on graphs with fast localized spectral filtering. In *Advances in Neural Information Processing Systems*, pages 3844–3852, 2016.
- [9] Hongyang Gao, Zhengyang Wang, and Shuiwang Ji. Large-scale learnable graph convolutional networks. In *Proceedings of the 24th ACM SIGKDD International Conference on Knowledge Discovery & Data Mining, KDD '18*, pages 1416–1424, New York, NY, USA, 2018. ACM.
- [10] Source code (as-gcn). <https://github.com/huangwb/AS-GCN>, 2019.
- [11] Source code (fastgcn). <https://github.com/matenure/FastGCM>, 2019.
- [12] Source code (graphsage). <https://github.com/williamleif/GraphSAGE>, 2019.
- [13] Source code (s-gcn). https://github.com/thu-ml/stochastic_gcn, 2019.
- [14] Will Hamilton, Zitao Ying, and Jure Leskovec. Inductive representation learning on large graphs. In *Advances in Neural Information Processing Systems 30*, pages 1024–1034. 2017.
- [15] Kaiming He, Xiangyu Zhang, Shaoqing Ren, and Jian Sun. Deep residual learning for image recognition. *CoRR*, abs/1512.03385, 2015.
- [16] Sepp Hochreiter and Jürgen Schmidhuber. Long short-term memory. *Neural computation*, 9(8):1735–1780, 1997.

- [17] Pili Hu and Wing Cheong Lau. A survey and taxonomy of graph sampling. *arXiv preprint arXiv:1308.5865*, 2013.
- [18] Wenbing Huang, Tong Zhang, Yu Rong, and Junzhou Huang. Adaptive sampling towards fast graph representation learning. In *Advances in Neural Information Processing Systems*, pages 4558–4567, 2018.
- [19] Diederik P Kingma and Jimmy Ba. Adam: A method for stochastic optimization. *arXiv preprint arXiv:1412.6980*, 2014.
- [20] Thomas N. Kipf and Max Welling. Semi-supervised classification with graph convolutional networks. *CoRR*, abs/1609.02907, 2016.
- [21] Johannes Klicpera, Aleksandar Bojchevski, and Stephan Günnemann. Personalized embedding propagation: Combining neural networks on graphs with personalized pagerank. *CoRR*, abs/1810.05997, 2018.
- [22] John Boaz Lee, Ryan A. Rossi, Xiangnan Kong, Sungchul Kim, Eunye Koh, and Anup Rao. Higher-order graph convolutional networks. *CoRR*, abs/1809.07697, 2018.
- [23] Jure Leskovec and Christos Faloutsos. Sampling from large graphs. In *Proceedings of the 12th ACM SIGKDD international conference on Knowledge discovery and data mining*, pages 631–636. ACM, 2006.
- [24] R. Li, J. X. Yu, L. Qin, R. Mao, and T. Jin. On random walk based graph sampling. In *2015 IEEE 31st International Conference on Data Engineering*, pages 927–938, April 2015.
- [25] Nus-wide datasets. <http://lms.comp.nus.edu.sg/research/NUS-WIDE.htm>, 2019.
- [26] Bruno Ribeiro and Don Towsley. Estimating and sampling graphs with multidimensional random walks. In *Proceedings of the 10th ACM SIGCOMM conference on Internet measurement*, pages 390–403. ACM, 2010.
- [27] Ppi/reddit datasets. <http://snap.stanford.edu/graphsage/#datasets>, 2019.
- [28] Flickr datasets. <https://snap.stanford.edu/data/web-flickr.html>, 2019.
- [29] Petar Veličković, Guillem Cucurull, Arantxa Casanova, Adriana Romero, Pietro Lio, and Yoshua Bengio. Graph attention networks. *arXiv preprint arXiv:1710.10903*, 2017.
- [30] Zonghan Wu, Shirui Pan, Fengwen Chen, Guodong Long, Chengqi Zhang, and Philip S. Yu. A comprehensive survey on graph neural networks. *CoRR*, abs/1901.00596, 2019.
- [31] Keyulu Xu, Chengtao Li, Yonglong Tian, Tomohiro Sonobe, Ken-ichi Kawarabayashi, and Stefanie Jegelka. Representation learning on graphs with jumping knowledge networks. *arXiv preprint arXiv:1806.03536*, 2018.
- [32] Yelp 2018 challenge. <https://www.yelp.com/dataset>, 2019.
- [33] Rex Ying, Ruining He, Kaifeng Chen, Pong Eksombatchai, William L. Hamilton, and Jure Leskovec. Graph convolutional neural networks for web-scale recommender systems. In *Proceedings of the 24th ACM SIGKDD International Conference on Knowledge Discovery & Data Mining*, KDD ’18, 2018.
- [34] Rex Ying, Jiaxuan You, Christopher Morris, Xiang Ren, William L. Hamilton, and Jure Leskovec. Hierarchical graph representation learning with differentiable pooling. In *Proceedings of the 32Nd International Conference on Neural Information Processing Systems*, NIPS’18, pages 4805–4815, USA, 2018. Curran Associates Inc.
- [35] Hanqing Zeng, Hongkuan Zhou, Ajitesh Srivastava, Rajgopal Kannan, and Viktor K. Prasanna. Accurate, efficient and scalable graph embedding. *CoRR*, abs/1810.11899, 2018.
- [36] Zhenpeng Zhou. Graph convolutional networks for molecules. *CoRR*, abs/1706.09916, 2017.
- [37] Marinka Zitnik and Jure Leskovec. Predicting multicellular function through multi-layer tissue networks. *CoRR*, abs/1707.04638, 2017.

A Proofs

Proof of Proposition 3.1. Under the condition that v is sampled in a subgraph:

$$\begin{aligned}
\mathbb{E} \left(\zeta_v^{(\ell+1)} \right) &= \mathbb{E} \left(\sum_{u \in \mathcal{V}} \frac{\tilde{\mathbf{A}}_{v,u}}{\alpha_{u,v}} \tilde{\mathbf{x}}_u^{(\ell)} \mathbb{1}_{u|v} \right) \\
&= \sum_{u \in \mathcal{V}} \frac{\tilde{\mathbf{A}}_{v,u}}{\alpha_{u,v}} \tilde{\mathbf{x}}_u^{(\ell)} \mathbb{E} \left(\mathbb{1}_{u|v} \right) \\
&= \sum_{u \in \mathcal{V}} \frac{\tilde{\mathbf{A}}_{v,u}}{\alpha_{u,v}} \tilde{\mathbf{x}}_u^{(\ell)} P \left((u, v) \text{ sampled} \mid v \text{ sampled} \right) \\
&= \sum_{u \in \mathcal{V}} \frac{\tilde{\mathbf{A}}_{v,u}}{\alpha_{u,v}} \tilde{\mathbf{x}}_u^{(\ell)} \frac{P \left((u, v) \text{ sampled} \right)}{P \left(v \text{ sampled} \right)} \\
&= \sum_{u \in \mathcal{V}} \frac{\tilde{\mathbf{A}}_{v,u}}{\alpha_{u,v}} \tilde{\mathbf{x}}_u^{(\ell)} \frac{p_{u,v}}{p_v}
\end{aligned} \tag{5}$$

where the second equality is due to linearity of expectation, and the third equality (conditional edge probability) is due to the initial condition that v is sampled in a subgraph.

It directly follows that, when $\alpha_{u,v} = \frac{p_{u,v}}{p_v}$,

$$\mathbb{E} \left(\zeta_v^{(\ell+1)} \right) = \sum_{u \in \mathcal{V}} \tilde{\mathbf{A}}_{v,u} \tilde{\mathbf{x}}_u^{(\ell)}$$

□

Proof of Theorem 3.2. Below, we use $\text{Cov}(\cdot)$ to denote covariance and $\text{Var}(\cdot)$ to denote variance. For independent edge sampling as defined in Section 3.3, $\text{Cov} \left(\mathbb{1}_{e_1}^{(\ell_1)}, \mathbb{1}_{e_2}^{(\ell_2)} \right) = 0, \forall e_1 \neq e_2$. And for a full GCN on the subgraph, $\text{Cov} \left(\mathbb{1}_e^{(\ell_1)}, \mathbb{1}_e^{(\ell_2)} \right) = p_e - p_e^2$. Therefore,

$$\begin{aligned}
\text{Var}(\zeta) &= \sum_{e, \ell} \left(\frac{b_e^{(\ell)}}{p_e} \right)^2 \text{Var} \left(\mathbb{1}_e^{(\ell)} \right) + 2 \sum_{e, \ell_1, \ell_2} \frac{b_e^{(\ell_1)} b_e^{(\ell_2)}}{p_e^2} \text{Cov} \left(\mathbb{1}_e^{(\ell_1)}, \mathbb{1}_e^{(\ell_2)} \right) \\
&= \sum_{e, \ell} \frac{(b_e^{(\ell)})^2}{p_e} - \sum_e (b_e^{(\ell)})^2 + 2 \sum_{e, \ell_1, \ell_2} \frac{b_e^{(\ell_1)} b_e^{(\ell_2)}}{p_e^2} (p_e - p_e^2) \\
&= \sum_e \frac{\left(\sum_{\ell} b_e^{(\ell)} \right)^2}{p_e} - \sum_e \left(\sum_{\ell} b_e^{(\ell)} \right)^2
\end{aligned} \tag{6}$$

Let a given constant $m = \sum_e p_e$ be the expected number of sampled edges. By Cauchy-Schwarz inequality: $\sum_e \frac{(\sum_{\ell} b_e^{(\ell)})^2}{p_e} m = \sum_e \left(\frac{\sum_{\ell} b_e^{(\ell)}}{\sqrt{p_e}} \right)^2 \sum_e (\sqrt{p_e})^2 \geq \left(\sum_{e, \ell} b_e^{(\ell)} \right)^2$. The equality is achieved when $\sum_{\ell} b_e^{(\ell)} / \sqrt{p_e} \propto \sqrt{p_e}$. i.e., variance is minimized when $p_e \propto \sum_{\ell} b_e^{(\ell)}$.

It directly follows that:

$$p_e = \frac{m}{\sum_{e', \ell} b_{e'}^{(\ell)}} \sum_{\ell} b_e^{(\ell)}$$

□

Algorithm 2 Graph sampling algorithms by GraphSAINT

Input: Training graph $\mathcal{G}(\mathcal{V}, \mathcal{E})$; Sampling parameters: node budget n ; edge budget m ; number of roots r ; random walk length h

Output: Sampled graph $\mathcal{G}_s(\mathcal{V}_s, \mathcal{E}_s)$

```
1: function NODE( $\mathcal{G}, n$ ) ▷ Node sampler
2:    $P(v) := \left\| \tilde{\mathbf{A}}_{:,v} \right\|^2 / \sum_{v' \in \mathcal{V}} \left\| \tilde{\mathbf{A}}_{:,v'} \right\|^2$ 
3:    $\mathcal{V}_s \leftarrow n$  nodes randomly sampled (with replacement) from  $\mathcal{V}$  according to  $P$ 
4:    $\mathcal{G}_s \leftarrow$  Node induced subgraph of  $\mathcal{G}$  from  $\mathcal{V}_s$ 
5: end function
6: function EDGE( $\mathcal{G}, m$ ) ▷ Edge sampler (approximate version)
7:    $P((u, v)) := \left( \frac{1}{\deg(u)} + \frac{1}{\deg(v)} \right) / \sum_{(u', v') \in \mathcal{E}} \left( \frac{1}{\deg(u')} + \frac{1}{\deg(v')} \right)$ 
8:    $\mathcal{E}_s \leftarrow m$  edges randomly sampled (with replacement) from  $\mathcal{E}$  according to  $P$ 
9:    $\mathcal{V}_s \leftarrow$  Set of nodes that are end-points of edges in  $\mathcal{E}_s$ 
10:   $\mathcal{G}_s \leftarrow$  Node induced subgraph of  $\mathcal{G}$  from  $\mathcal{V}_s$ 
11: end function
12: function RW( $\mathcal{G}, r, h$ ) ▷ Random walk sampler
13:   $\mathcal{V}_{\text{root}} \leftarrow r$  nodes sampled uniformly at random (with replacement) from  $\mathcal{V}$ 
14:   $\mathcal{V}_s \leftarrow \mathcal{V}_{\text{root}}$ 
15:  for  $v \in \mathcal{V}_{\text{root}}$  do
16:     $u \leftarrow v$ 
17:    for  $d = 1$  to  $h$  do
18:       $u \leftarrow$  Node sampled uniformly at random from  $u$ 's neighbor
19:       $\mathcal{V}_s \leftarrow \mathcal{V}_s \cup \{u\}$ 
20:    end for
21:  end for
22:   $\mathcal{G}_s \leftarrow$  Node induced subgraph of  $\mathcal{G}$  from  $\mathcal{V}_s$ 
23: end function
24: function MRW( $\mathcal{G}, n, r$ ) ▷ Multi-dimensional random walk sampler
25:   $\mathcal{V}_{\text{FS}} \leftarrow r$  nodes sampled uniformly at random (with replacement) from  $\mathcal{V}$ 
26:   $\mathcal{V}_s \leftarrow \mathcal{V}_{\text{FS}}$ 
27:  for  $i = r + 1$  to  $n$  do
28:    Select  $u \in \mathcal{V}_{\text{FS}}$  with probability  $\deg(u) / \sum_{v \in \mathcal{V}_{\text{FS}}} \deg(v)$ 
29:     $u' \leftarrow$  Node randomly sampled from  $u$ 's neighbor
30:     $\mathcal{V}_{\text{FS}} \leftarrow (\mathcal{V}_{\text{FS}} \setminus \{u\}) \cup \{u'\}$ 
31:     $\mathcal{V}_s \leftarrow \mathcal{V}_s \cup \{u\}$ 
32:  end for
33:   $\mathcal{G}_s \leftarrow$  Node induced subgraph of  $\mathcal{G}$  from  $\mathcal{V}_s$ 
34: end function
```

B Sampling Algorithm

Algorithm 2 lists the four graph samplers we have integrated into GraphSAINT. The naming of the samplers follows that in Table 2. Note that the sampling parameters n and m specify a budget rather than the actual number of nodes and edges in the subgraph \mathcal{G}_s . Since certain nodes or edges in the training graph \mathcal{G} are more likely to be sampled, we often have $|\mathcal{V}_s| < n$ for node and MRW samplers, $|\mathcal{V}_s| < 2m$ for edge sampler, and $|\mathcal{V}_s| < r \cdot h$ for RW sampler.

Also note that the edge sampler presented in Algorithm 2 is an approximate version of the original algorithm in Section 3.4. The complexity (excluding the subgraph induction step) of the original version in Section 3.4 is $\mathcal{O}(|\mathcal{E}|)$, while the complexity of the approximate one is $\mathcal{O}(m)$. As long as $m \ll |\mathcal{E}|$, the approximate version leads to the same accuracy as the original one, under a given m .

C Detailed Experimental Setup

C.1 Hardware Specification and Environment

We run our experiments on a single machine with Dual Intel Xeon CPUs (E5-2698 v4 @ 2.2Ghz), one NVIDIA Tesla P100 GPU (16GB of HBM2 memory) and 512GB of DDR4 memory. The code is written in Python 3.6.8 (where the sampling part is written with Cython 0.29.2). We use Tensorflow 1.12.0 on CUDA 9.2 with CUDNN 7.2.1 to train the model on GPU. Since the subgraphs are sampled independently, we run the sampler in parallel with 20 CPU cores.

C.2 Additional Dataset Details

Here we present the detailed procedures to prepare the Yelp and Flickr datasets.

The Yelp dataset is provided with raw json data of businesses, users and reviews [32]. For nodes and edges, we scan the friends list of each user in the raw json file of users. If two users are friends, we create an edge between the nodes representing the two users. We then filter out all the reviews by each user and separate the reviews into words. Each review word is converted to a 300-dimensional vector using the Word2Vec model pre-trained on GoogleNews[†]. The word vectors of each node are added and normalized to serve as the node feature (i.e., x_v). As for the node labels, we scan the raw json file of businesses, and use the categories of the businesses reviewed by a user v as the multi-class label of v .

The Flickr dataset originates from NUS-wide [25]. The website [28] collected Flickr data from four different sources including NUS-wide, and generated an un-directed graph. One node in the graph represents one image uploaded to Flickr. If two images share some common property (e.g., same geographic location, same gallery, comments by the same user, etc.), there is an edge between the nodes of these two images. We remove the nodes of [28] that do not appear in the NUS-wide dataset. We directly use the 500-dimensional bag-of-word representation of the images provided by [25] as the node features. For labels, we scan over the 81 tags of each image and manually merged them to 7 classes. Each image belongs to one of the 7 classes.

D Additional Experimental Configuration

The optimizer for GraphSAINT and all baselines is Adam [19]. We sweep the hidden dimensions for all five baselines from 128 to 512. We find out that hidden dimensions of 512 (PPI), 256 (Flickr), 128 (Reddit) and 512 (Yelp) lead to the best accuracy for most baselines. To make fair comparison, GraphSAINT also uses the same dimensions for these datasets. We also test dropout of 0, 0.1, 0.2 and 0.3 for GraphSAINT and each baseline separately and report results corresponding to the configuration with better accuracy. All accuracy and training time results are averaged from three runs without fixing random seed.

Note that we report execution time rather than number of epochs. The reason is that in graph sampling based minibatch training, there lacks a clear definition of “one epoch” — there is no guarantee that certain number of subgraphs will cover all the training nodes exactly once.

All the five baselines terminate after a fixed number of epochs based on convergence, and GraphSAINT terminates after a fixed number of iterations (i.e., number of subgraphs). Note that [6, 5, 18] have also implemented an optional early stopping criteria based on loss. However, such early stopping sometimes terminates training before the actual convergence. For example, S-GCN [5] on PPI may stop at around 0.6 F1-micro score based on their early stopping, while at the actual convergence it reaches 0.96 F1-micro score (as shown in Table 2). We thus consider these as abnormal points and do not include the early stopping results in Table 2.

For vanilla GCN [20] and AS-GCN [18], we set the batch size to their default value 512. For GraphSAGE [14], we use the mean aggregator with the default batch size 512. For S-GCN [5], we set the flag `-cv -cvd` (which stand for “control variate” and “control variate dropout”) with pre-computation of the first layer aggregation. According to their paper [5], such pre-computation significantly reduces training time without affecting accuracy. However, the benefit of pre-computation on

[†]<https://code.google.com/archive/p/word2vec/>

Table 3: Training configuration of GraphSAINT for Table 2

Method	Dataset	Training		Sampling			
		Learning rate	Dropout	Node budget	Edge budget	Roots	Walk length
Node	PPI	0.01	0.0	6000	—	—	—
	Flickr	0.01	0.2	8000	—	—	—
	Reddit	0.01	0.1	8000	—	—	—
	Yelp	0.01	0.1	5000	—	—	—
Edge	PPI	0.01	0.1	—	4000	—	—
	Flickr	0.01	0.2	—	6000	—	—
	Reddit	0.01	0.1	—	6000	—	—
	Yelp	0.01	0.1	—	2500	—	—
RW	PPI	0.01	0.1	—	—	3000	2
	Flickr	0.01	0.2	—	—	6000	2
	Reddit	0.01	0.1	—	—	2000	4
	Yelp	0.01	0.1	—	—	1250	2
MRW	PPI	0.01	0.1	8000	—	2500	—
	Flickr	0.01	0.2	12000	—	3000	—
	Reddit	0.01	0.1	8000	—	1000	—
	Yelp	0.01	0.1	2500	—	1000	—

Table 4: Training configuration of GraphSAINT for Figure 4 (Reddit; Edge sampler)

	2-layer GCN	4-layer JK-Net
Hidden dimension	128	128
Aggregation \oplus	—	Concat.
Edge budget	6000	11000
Learning rate	0.01	0.01
Dropout	0.1	0.2

training time diminishes for deeper GCN models. Thus, we choose not to integrate it in GraphSAINT, even though such idea is applicable to graph sampling based training. For S-GCN [5] and FastGCN [6], the Table 2 results correspond to their default batch size of 1000 (for [5]) and 400 (for [6]). In addition, we are aware of the following: 1. Accuracy of FastGCN may improve under larger batch sizes, due to better connectivity among sampled nodes, and 2. Training time of S-GCN may decrease under larger batch sizes due to higher GPU utilization. Therefore, we conduct additional experiments on these two baselines with larger batch sizes. See Table 5 in the next section for details.

Configuration of GraphSAINT to reproduce Table 2 results is shown in Table 3. In Section 3.4, analysis suggests that we set the random walk length to be GCN depth when using “RW” sampler. In practice, we observe that sometimes increasing the walk length may lead to slightly better accuracy.

Below we describe the configuration for Figure 4. The major difference between a normal GCN and a JK-Net [31] is that JK-Net has an additional final layer that aggregates all the output hidden features of graph convolutional layers 1 to L . Mathematically, the additional aggregation layer outputs the final embedding \mathbf{x}_{JK} as follows (where based on [31], \oplus is the vector aggregation operator: max-pooling, concatenation or LSTM [16] based aggregation):

$$\mathbf{x}_{JK} = \sigma \left(\mathbf{W}_{JK}^T \cdot \bigoplus_{\ell=1}^L \mathbf{x}_v^{(\ell)} + \mathbf{b}_{JK} \right) \quad (7)$$

Table 4 shows the configuration of the two curves in Figure 4.

Table 5: Test set accuracy and training time for FastGCN and S-GCN under various batch sizes

Method	Batch size	PPI		Flickr		Reddit		Yelp	
		F1 _{mic}	Time (s)						
FastGCN [6]	400	0.513	7	0.504	82	0.924	400	0.265	744
	2000	0.561	12	0.506	142	0.934	477	0.255	1053
	4000	0.564	17	0.507	138	0.934	574	0.260	1464
S-GCN [5]	1000	0.963	40	0.464	8	0.964	119	0.640	117
	2000	0.646	12	0.485	12	0.949	86	0.614	69
	4000	0.804	30	0.482	4	0.949	86	0.594	60
	8000	0.694	16	0.483	13	0.950	96	0.613	76

E Additional Experiments

Table 5 shows additional experimental results on FastGCN [6] and S-GCN [5]. Except batch size, all other configurations are the same as those in Table 2. For FastGCN, while increasing the batch size may lead to better connected minibatches, such hyper-parameter tuning does not significantly help with accuracy improvement. When increasing batch size from 400 to 2000, we observe accuracy improvement on PPI, Flickr and Reddit, and accuracy degradation on Yelp. When further increasing the batch from 2000 to 4000, the accuracy stabilizes. For S-GCN, as expected, increasing batch size from the default value of 1000 shortens the GPU training time for some datasets. However, larger batch sizes also result in significant accuracy degradation. Therefore, we conclude that the default batch size of S-GCN still leads to the best overall performance.

On the other hand, using proper graph sampling algorithm, accuracy of GraphSAINT is not sensitive to the subgraph size, as shown in Figure 5.